Journal of Materials Chemistry A

REVIEW

View Article Online
View Journal | View Issue

CrossMark click for updates

Cite this: J. Mater. Chem. A, 2015, 3, 9020

Nanocarbons for mesoscopic perovskite solar cells

Munkhbayar Batmunkh,[ab] Cameron J. Shearer,[b] Mark J. Biggs[ac] and Joseph G. Shapter*[b]

Received 3rd February 2015
Accepted 9th February 2015

DOI: 10.1039/c5ta00873e

www.rsc.org/MaterialsA

Organic–inorganic halides based perovskite solar cells (PSCs) have attracted a great deal of attention from the photovoltaic (PV) research community due to the extremely rapid increases in efficiencies observed over the past few years. The PSC is an extension of dye-sensitised solar cells and has reached an energy conversion efficiency of 19.3% by mid-2014. However, PSCs do have some disadvantages such as use of expensive metal electrodes, the high temperature required during production and poor stability when in use. There is no doubt that research with carbon nanomaterials will play an important role in understanding and solving the issues currently observed in PSCs, as they consistently have been shown to improve performance in a wide range of energy related applications. The present review (i) provides a brief introduction to PSC development; (ii) highlights the notable achievements of PSCs; (iii) particularly focuses on the use of nanocarbon in mesoscopic PSCs and (iv) predicts and suggests a roadmap for the future application of carbon materials in this emerging technology.

1 Introduction

It is now widely accepted that direct conversion of the sun's energy into electricity is an unlimited clean and renewable resource that has great potential to address increasing energy demands and environmental pollution issues.[1,2] The challenge for renewable solar energy conversion is to reduce production cost and maximise efficiency. At present, almost ~90% of the commercial photovoltaic (PV) production is based on crystalline silicon (Si) solar cells which can deliver a power conversion

[a]School of Chemical Engineering, The University of Adelaide, Adelaide, South Australia 5005, Australia. E-mail: munkhbayar.batmunkh@adelaide.edu.au
[b]Centre for Nanoscale Science and Technology, School of Chemical and Physical Sciences, Flinders University, Bedford Park, Adelaide, South Australia 5042, Australia. E-mail: joe.shapter@flinders.edu.au; cameron.shearer@flinders.edu.au
[c]School of Science, Loughborough University, Loughborough, Leicestershire, LE11 3TU, UK. E-mail: m.biggs@lboro.ac.uk

Munkhbayar Batmunkh (referred as B. Munkhbayar) is currently a Ph.D. candidate (Australian Government and University sponsored student) at School of Chemical Engineering in the University of Adelaide, Australia. He is also a visiting researcher at School of Chemical and Physical Sciences in the Flinders University of South Australia. He obtained his "B.Sc. in Chemistry" from the National University of Mongolia, Mongolia, in 2010. Then, he completed his "Masters of Engineering" degree at Gyeongsang National University, South Korea, in 2012. His current research interests involve the modification and characterization of carbon nanotubes and graphene structures for use in dye-sensitized solar cells and perovskite solar cells.

Cameron Shearer obtained his PhD in 2012 at the Flinders University of South Australia where his work involved creating nanostructured surfaces for field emission, filtration/separation and cell growth. From 2012–2014 he worked as a post-doctoral research associate at the Westfälische Wilhelms-Universität Münster working on the fabrication of nanocarbon hybrids for a photocatalytic energy conversion and fundamental studies. He is currently a postdoctoral research associate at Flinders University and his research interests include the fabrication of new materials for energy conversion and advanced microscopy for nanoscale investigation of surface topography and electrochemical activity.

efficiency (PCE) of approximately 20% under full-sun illumination.[3] However, these Si-based PV cells suffer from high production costs and complicated manufacturing processes. As emerging PVs, several classes of technologies such as dye-sensitised solar cells (DSSCs),[4] organic PVs (OPVs),[5] inorganic cells (CZTSSe)[6] and quantum dot solar cells (QDSCs)[7] have been developed with the aim of replacing conventional Si-solar cells. Although these alternative PVs have been well explored (for at least 10 years), the improvements in PCEs have been relatively slow and have reached maximum efficiencies of only around 9.2–13% (Fig. 1a).[8–12] In addition, despite vast research efforts over the last decade, the PCEs achieved for these solar cells are still far from the target efficiency of 20%. Therefore, a more innovative and efficient solar energy conversion system that can be fabricated at reasonable cost is desired.

Perovskite solar cells (PSCs) evolved from DSSCs and are a new class of PV technology that have great potential to replace current commercial solar cells. A typical mesoscopic PSC is constructed using a transparent conductive oxide (TCO) film (usually fluorine doped tin oxide (FTO)), a thin, dense compact semiconducting layer that prevents short circuits, a mesoporous nanocrystalline semiconducting oxide layer, a light harvesting perovskite layer, a hole-transporting material (HTM) and a metal electrode (Au or Ag), as illustrated in Fig. 2a.[13] The entire working principles of PSCs have not been satisfactorily explained and can be different depending on the exact PSC structure. It is accepted that in the case of typical PSCs: upon illumination, the perovskite layer is excited, producing an electron–hole pair. The charge carriers can then diffuse to an interface where the electrons are injected into the conduction band of the semiconducting material whilst the holes are transported to the valence band of the HTM. Finally, the electrons and holes are then collected by the conductive electrodes.

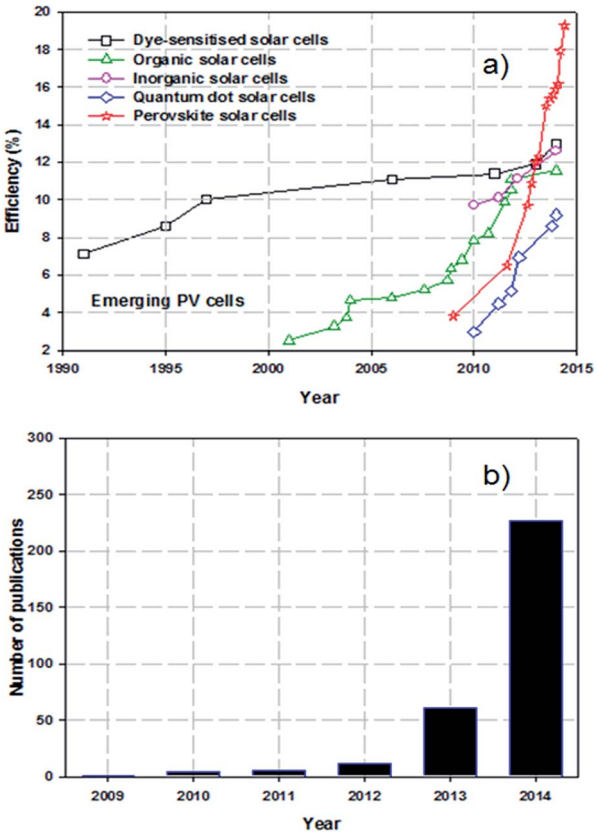

Fig. 1 (a) Efficiency records *vs.* year of third generation (emerging) PVs. The red line indicates that the efficiency of PSCs has improved dramatically in the past 2 years. (b) Number of publications (since 2009) that appeared in Scopus on 28th September, 2014. Keyword used in the search was "Perovskite Solar Cells" in the title of the article.

Mark Biggs, who received his PhD in 1996 from The University of Adelaide (Australia) in Chemical Engineering, is the Professor of Interfacial Science and Engineering and Dean of Science at Loughborough University in the UK. He is also a visiting professor at The University of Adelaide where he was until recently Professor of Chemical Engineering and Head of the School of Chemical Engineering. Previous to that he held positions in chemical engineering at The University of Edinburgh and Surrey University, both also in the UK. He is also a Fellow of the Institute of Engineers Australia, a Fellow of the Institute of Chemical Engineers (UK), and a Member of the Royal Australian Chemical Institute. Professor Biggs research interests are focused on understanding and exploiting interfacial phenomena, with particular (although not exclusive) interest in carbon-based materials.

Joe Shapter obtained his Ph. D. from the University of Toronto in 1990 working on the detection of small molecules and the determination of their energies. From 1990 to 1996, he worked at the University of Western Ontario (London, Ontario) building a scanning tunnelling microscope and lecturing first year chemistry. In 1996 he moved to Flinders and is now Professor of Nanotechnology and Dean of the School of Chemical and Physical Sciences. He was the founding Director of the Defence Science and Technology Organisation (DSTO) funded Centre of Expertise in Energetic Materials (CEEM) and is currently the Director of the South Australian node of the Australian Microscopy and Microanalysis Facility (AMMRF). His research interests lie in the use of carbon nanotubes for various applications including the production of novel photovoltaic systems.

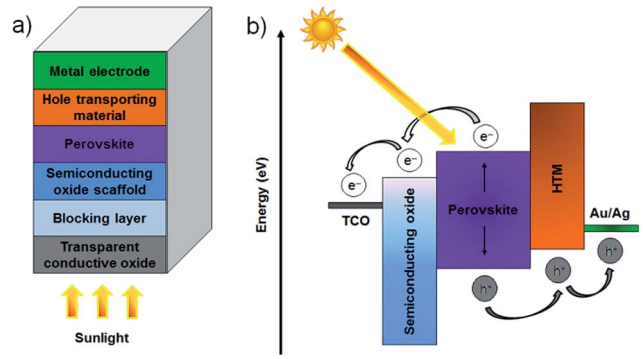

Fig. 2 (a) Structure and (b) operational mechanism of a typical PSC.

The process is thermodynamically favourable when the valence and conduction band energy levels of the layers align such that the electron transport proceeds to a lower energy level whilst hole transport proceeds to higher energy levels (see Fig. 2b). During the process, the compact layer prevents shunting and leakage of the current under reverse bias. Organometal trihalide perovskite materials, $CH_3NH_3PbX_3$ (X = Cl, Br, I), are implemented as the light absorber because of their broad and strong light absorption properties.

Perovskite based solar cells have attracted great attention from the PV research community due to their extraordinary light-harvesting characteristics.[14] A search of the online database Scopus, plotted in Fig. 1b, shows the very rapid increase in the number of publications on PSCs. The exponential growth in publication rate is a testament to both the performance and ease of manufacture of PSCs. Over the past two years, the implementation of organic–inorganic lead halide perovskite based light absorbers into solid-state solar cells has brought breakthroughs in low-cost PVs. Interestingly, the progress of state of the art PSCs has been astounding and the highest energy conversion efficiency of 19.3% was recently reached (Fig. 1a).[24] A brief overview of notable achievements of PSCs is illustrated in Fig. 3, as they are previously summarised in several recent reviews.[25–37] Additionally, we describe the PSC structures that correspond to each published efficiency record from 3.8% to 19.3% (Fig. 3). The general structure of PSCs have remained similar with improvements in efficiency related to the implementation a solid-state hole transporting material and the mixing of the perovskite within the mesoporous metal oxide layer.

Recent breakthroughs show PV cells based on perovskite light absorbers are approaching the efficiency of commercially available Si-based solar cells.[23,24] PSCs have several advantages such as remarkably high efficiency along with a simple and low cost synthesis. However, they also suffer from several drawbacks namely: (i) use of expensive, rare materials, (ii) high-temperature processing of n-type TiO_2 layer, (iii) relatively slow electron transport between the perovskite and TiO_2 and (iv) a lack of long-term stability. Consequently, it is necessary to overcome these issues in order to make this novel high efficiency solar cell commercially viable. Very recently, carbon nanomaterials, with their excellent conductivity and good chemical stability, have

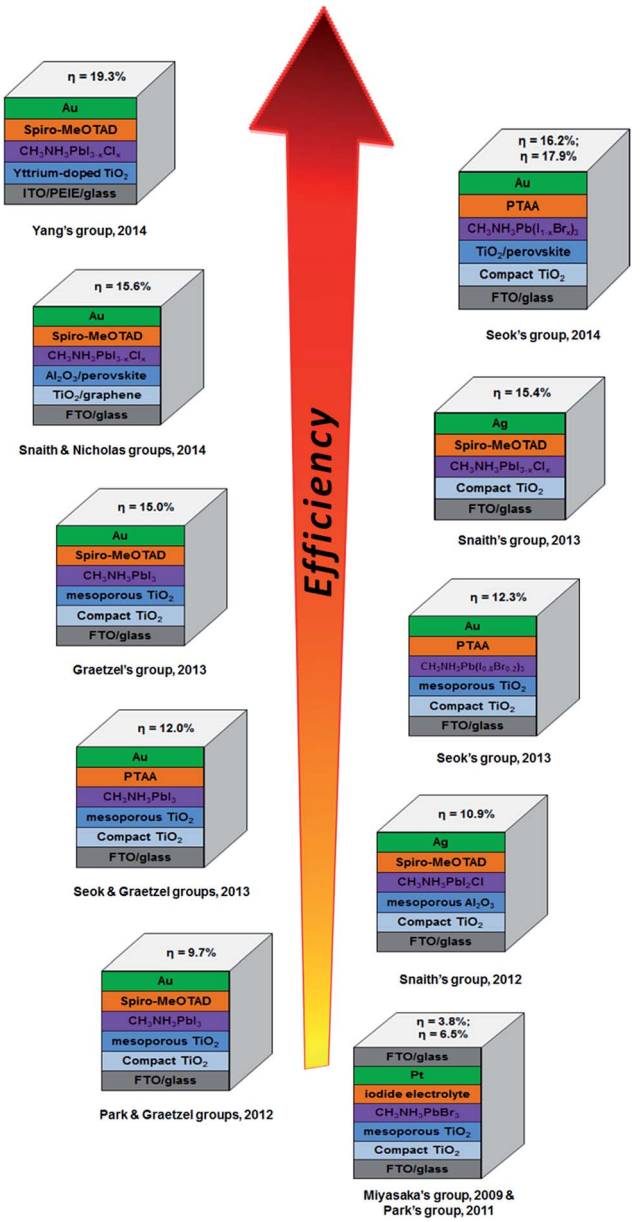

Fig. 3 Progress in the efficiency record of PSCs since 2009 showing the structures of PSCs (constructed by the corresponding groups) used to achieve the reported energy conversion efficiencies. These PSCs have been reported in ref. 13–24.

been applied in PSCs to tackle the aforementioned bottlenecks. Moreover, it should be noted that one of the efficiency records (15.6% in Fig. 3) of PSCs was achieved by the use of graphene (member of carbon family).[21] This clearly indicates that carbon materials are very promising candidates for the development of this emerging technology.

Furthermore, it is no surprise that carbonaceous materials including carbon particles, carbon nanotubes (CNTs) and graphene would have significant role in the development of PSCs as they have been extensively studied in various energy related applications owing to their excellent properties, low cost and abundance.[38–57] Since mid-2013, tremendous efforts have been

made in the use of carbon materials in the mesoscopic PSCs. Because of this rapidly growing research interest in this advancing field, emphasising their past discoveries, achievements and developments is of great importance.

Herein, we contribute to this cutting-edge research area by providing a review that focuses on the successful application of carbon nanomaterials for perovskite-based low cost PV cells. There is little doubt that the use of carbonaceous materials will advance the PV performance of PSCs whilst maintaining low production cost.

2 Carbon based PSCs

While a great deal of important work has been done on the use of carbonaceous materials in planar heterojunction PSCs,[58–63] this review will cover only the mesoscopic PSCs. The structure and operating principle of the two types of cells are very different and hence it is difficult to do justice to both architectures in one review. As shown in Fig. 2, the key components of the mesoscopic PSC are the back metal electrode, hole transporting layer (HTM), perovskite, semiconducting oxide scaffold, a blocking layer and the transparent conducting oxide. Carbon nanomaterials have been used in several of these layers and this work will be discussed in the following. The potential use of carbon nanomaterials in other sections of PSC will then be discussed.

2.1 Successful applications of carbon materials in PSCs

Back contact layer (metal electrodes). Thin layers of noble metals such as gold (Au) or silver (Ag) prepared by thermal evaporation are used as the back contact in PSCs. However, the use of the thermal evaporation process involves inherently complicated vacuum technologies. More importantly, the costs of metal electrode and its coating techniques are relatively high and would limit large-scale production of PSCs. Therefore, the replacement of this precious metal electrode with other low cost materials that are abundantly available and can exhibit high performance is urgently required for this class of solar cells. Undoubtedly, carbonaceous materials are very promising candidates to replace the expensive metals in PSCs as they have shown comparable or even better performance in many other types of solar cells. Not only have they exhibited good performance, they also afford PV devices which are flexible and semi-transparent. Carbon nanomaterials are low-cost materials and abundant and they possess good chemical stability, excellent conductivity and suitable energy levels for PSCs. Taking benefits from these unique properties, several groups have applied different types of carbonaceous structures as the substitution of metal cathode in PSCs.

To the best of our knowledge, Han's group[64] was the first to report the implementation of carbon materials in the counter electrode of $CH_3NH_3PbI_3$ based PSCs. They deposited a carbon black/graphite composite *via* screen printing technique on the PSC photoelectrode that consisted of FTO glass substrate, TiO_2 compact layer, mesoporous TiO_2 layer and ZrO_2 spacer layer. Finally, the manufacturing process of the PSC was completed by drop-coating of $CH_3NH_3PbI_3$ perovskite sensitiser onto the mesoscopic carbon layer (see Fig. 4a). In the carbon black/graphite composite materials, two kinds of graphite (flaky and spheroidal graphite) were used and their PV performances were compared. The highest PCE (6.64%) was achieved by PSC assembled with the spheroidal graphite based carbon composite cathodes. One of the main reasons for this good performance by carbon cathode employed PSCs is, of course, the suitable energy levels of carbon material when compared with the other components of the device. In particular, upon exposure to sunlight, the perovskite sensitiser generates electrons and holes in the conduction band (−3.93 eV) and valence band (−5.43 eV), respectively. Since the conduction band of ZrO_2 is at −3.27 eV, the photo-generated electrons on $CH_3NH_3PbI_3$ conduction band are directly injected into the conduction band of TiO_2 (−4.0 eV) whilst the holes are transferred into the carbon (−5.0 eV) (energy levels shown in Fig. 4b).[64] On the other hand, these authors have also demonstrated that the application of carbon nanomaterials in the counter electrode of PSCs not only replaced precious metal, it can also avoid using expensive organic HTMs. It should be noted that the use of the organic HTMs (*e.g.* namely 2,2′,7,7′-tetrakis(*N*,*N*-di-*p*-methoxyphenylamine)-9,9′-spirobifluorene, Spiro-OMeTAD) has some drawbacks such as high material cost and poor stability. Interestingly, the initial efficiency (6.64%) of carbon cathode employed PSC still remained at high with a PCE value (above 6.5%) even after 840 h, shown in Fig. 4c. This result suggests that the use of carbon nanomaterials in the PSC cathode can simultaneously address several limitations of this high-performance PV device.

A series of studies have reported applying various carbon materials as PSC cathodes with the goal of improving efficiency after the initial report from Han's group.[65–73] The same group were able to further improve their previous efficiency (6.64%) to

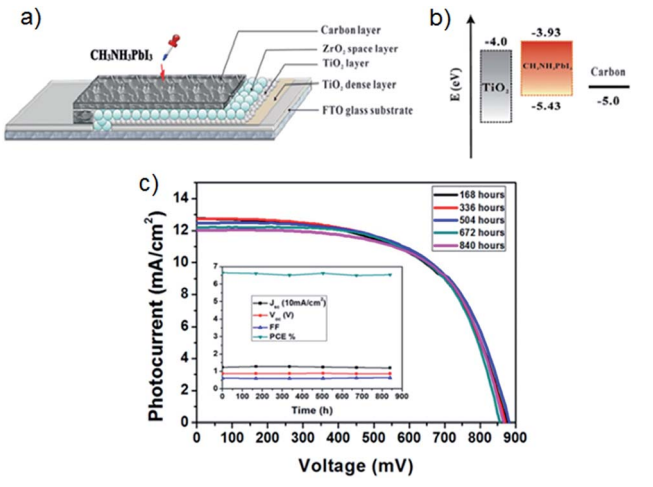

Fig. 4 (a) The structure of the first carbon counter electrode based PSC.[64] (b) Energy level of TiO_2, $CH_3NH_3PbI_3$ and carbon.[64] (c) Current density–voltage curves of carbon cathode based PSCs over 840 hours. Inset: the effect of time on each value (J_{sc}, V_{oc}, FF and PCE) of solar cell. Reprinted with permission from ref. 64 © 2013, Nature Publishing Group.

~10.6% [65] by using TiO_2 nanosheets on the photoelectrode and ~11.6% [67] by optimising the thickness of the carbon counter electrodes. In their latest work,[67] they explored the influence of the thickness of carbon black/graphite film (3–15 μm) on the cell performance. The best efficiency of the PSCs was achieved by employing a carbon black/graphite counter electrode with an optimised thickness of 9 μm. Meanwhile, the collaborative work of Han's and Graetzel's group reported the fabrication of hole-conductor-free and fully printable PSCs.[68] Indeed, this work achieved the highest efficiency to date of carbonaceous cathode based cells. The manufacturing process of this porous carbon cathode based cell was unique in that it used 5-ammoniumvaleric acid (5-AVA) iodide based perovskite as a sensitiser. The 5-AVA played an important role in controlling the formation of perovskite crystals in the mesoporous oxide and providing better growth within the network. Consequently, the 5-AVA cations based perovskite provided good surface contact with the TiO_2 and lower defect concentration. Indeed, the measured short circuit current (J_{sc}), open circuit voltage (V_{oc}) and fill factor (FF) for this PSC which still used the carbonaceous cathode were 22.8 mA cm^{-2}, of 0.86 V and 0.66, respectively and yielded a PCE of 12.8%.[68]

Very recently, an interesting study was reported by Wei *et al.*,[70] who simply fabricated PSCs by clamping a mesoporous $TiO_2/CH_3NH_3PbI_3$ perovskite based photoelectrode to a candle-soot film. The candle soot film was prepared by holding FTO glass above the candle flame (see Fig. 5a). It can be seen from the scanning electron microscope (SEM) image in Fig. 5b that a loose sponge-like structure of candle soot was well assembled. The particle size of the candle soot was measured to be ~30 nm based on transmission electron microscope (TEM) images of the film (Fig. 5c). In order to fabricate high-performance PSCs using this candle soot film, the authors made several systematic attempts. Their first attempt (termed 1st generation) shown in Fig. 5d featured direct assembly of the photoelectrode with a candle-soot counter electrode. The cell fabricated *via* the 1st generation clamping method exhibited PV efficiency of only 2.6%. This inferior performance was due to the low conductivity of the as-prepared candle-soot film and poor contact between the perovskite and candle soot. The aim of the second attempt (termed 2nd generation) was to address these problems by annealing and rolling transfer of the candle-soot film (see Fig. 5d). The annealing process increased the conductivity of the film and the rolling transfer provided a better interface contact. By applying such treatment (2nd generation), the authors observed significant improvement in the PSC performance. However, this improved PCE (5.44%) was still considered unsatisfactory. The problem for the 2nd generation clamping was the non-ideal interface contact between perovskite and candle soot. So, the 3rd generation clamping, which involved a two-step method (shown in Fig. 5d) was designed to overcome this limitation. Finally, the best performing PSC fabricated with the candle-soot counter electrode was able to deliver an energy conversion efficiency of 11.02%. The simplicity of this approach coupled with the fact that two layers, the counter electrode and the HTM layer, are replaced with one layer makes this work very interesting in terms of future potential commercial production.

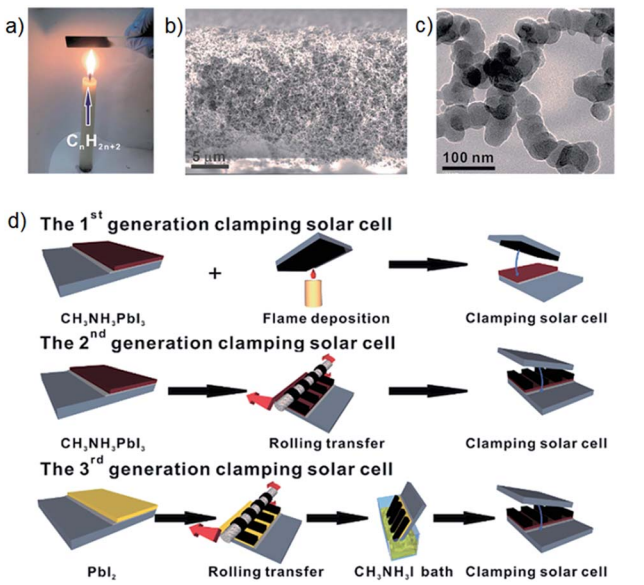

Fig. 5 (a) Digital photo of the candle-soot film preparation. (b) Cross sectional SEM image of the candle-soot film. (c) TEM image of the as-prepared candle-soot particles. (d) Fabrication processes of the candle-soot film based PSCs. Reprinted from ref. 70.

Li *et al.*[69] first reported CNT networks as the counter electrode of PSC. A reasonable comparison was made by these authors by fabricating HTM-free PSCs based on only CNTs or only Au electrode. In the absence of organic HTMs, the efficiency of CNTs cathode employed cell was 6.87% which was far higher than that (5.14%) achieved by the Au based device. This impressive result indicates that the use of CNTs can outperform those precious metal based PSCs. Furthermore, the efficiency of the PSC fabricated with CNTs cathode was improved to be 9.9% by adding spiro-OMeTAD. In addition to this improvement, excellent development in this class of solar cells could be achieved by upgrading the CNT properties. For instance, the use of chirality sorted nanotubes to give separated metallic CNTs would bring a critical improvement in the PSC performance because it enhances the charge selectivity.[74] Moreover, since chemically doped CNTs or graphene show excellent conductivity, they should exhibit very high charge extraction rate. Applying a chemical doping approach on the carbon nanomaterials could be promising way to further improve the solar cell performance.[75]

Very recently, the first fibre-shaped PSC was fabricated by Qiu *et al.*,[71] who used stainless steel wires with a TiO_2 compact layer and mesoporous layer as the anode, $CH_3NH_3PbI_3$ perovskite as the sensitiser, spiro-OMeTAD as the HTM and transparent CNTs as the cathode. The advantage of the fiber-shaped PSCs is that they are a lightweight and flexible device. Indeed, this first fibre-shaped PSC exhibited a good J_{sc} (~9.5 mA cm^{-2}) and yielded an energy conversion efficiency of 3.3% after optimisation. These authors believed that this good J_{sc} resulted from the high electrical conductivity of CNTs that provided a rapid charge transport.

Hole transporting layer. After photoexcitation of the perovskite layer, to reduce potential recombination, holes are extracted by the hole transporting layer. This is achieved using materials with suitable band positions such that the transport of holes is facilitated whilst the transport of electrons is thermodynamically unfavourable. Hole conductors, (spiro-OMeTAD), poly(triarylamine) (PTAA) and poly(3-hexylthiophene) (P3HT), have been demonstrated to be the best HTMs for the fabrication of high-performance PSCs.[13–24] In particular, spiro-OMeTAD is the most commonly employed HTM in solid-state solar cells including PSCs.[76–78] There are two main challenges for using spiro-OMeTAD: (i) limited long-term stability and (ii) high material cost. Therefore, exploring alternate cheaper materials that can show high stability whilst maintaining efficiency is of great interest. Very recently, a composite material based on CNTs and polymer has been used as a highly stable hole collection layer in PSCs as reported by Snaith's group.[79] They used an insulating hydrophobic polymer poly-(methylmethacrylate) (PMMA) because this polymer inhibits both the intrusion of moisture into the perovskite and the evaporation of the methylammonium iodide. By doing so, PMMA exhibited better stability compared to the conventional HTMs even after 96 h at 80 °C in air. However PMMA is insulating, subsequently the authors incorporated highly conductive CNTs[80] into the hole transporting layer of P3HT to efficiently transport the holes within the cells. Taking benefits from both the PMMA and CNTs, Snaith's group[79] was able to achieve an energy conversion efficiency of 15.3% using their unique PSCs depicted in Fig. 6a. This solar cell showed strong retardation in thermal degradation as compared to the conventional organic HTMs employed devices. It is worth noting that these PSCs exhibited an excellent stability not only under thermal stress but also their resistance to water ingress was also increased. Particularly, no significant change was observed in the cell performance before and after being placed under the running water for 1 min, as shown in Fig. 6b. Based on this study, it can be summarised that the presence of carbon materials (CNT/polymer hybrids in this work) has an important role in improving the stability of PSCs. Therefore, it can be expected that the application of additional treatments on CNTs and/or other types of carbonaceous structures will bring significant enhancement on this class of solar cells. Further work on the stability of PSCs should be conducted by applying functionalised CNT structures with other polymers. Moreover, the use of graphene or graphene oxide materials in the hole transporting layer of PSCs would be of great value.

Perovskite layer. In PSCs, perovskite sensitisers are used due to their superb light-harvesting characteristics. They play an important role in absorbing light to generate charges and injecting the electrons and holes into the conduction band of TiO_2 and valence band of HTM, respectively. Of particular concern here is the injection time of electrons to the TiO_2, with recombination reduced when the injection time is shorter. The electron injection time from the perovskite to the electron acceptor has been measured to be ~0.3 ns,[81] which can be considered too long compared to the measurement of the hot carrier cooling (or thermalisation) time (~0.4 ps).[82] Once again, carbon based materials could address this limitation of PSCs as they have shown an ultrafast electron injection to the TiO_2 interface.[83,84] To our knowledge, only two studies have used carbonaceous materials between perovskite and TiO_2 layers to improve the performance of PSCs.[81,85] The most recent example of the incorporation of nanocarbons into the photoactive layer applied graphene quantum dots (GQDs),[81] whilst the other one utilised a fullerene self-assembled monolayer (C_{60}SAM).[85]

The idea of incorporating nanocarbons between the perovskite layer and mesoporous semiconducting oxide layer was first initiated by Snaith's group by applying a C_{60}SAM upon the mesoporous TiO_2 layer.[85] They found that the C_{60}SAM acts as a very effective electron acceptor from both the perovskite and P_3HT polymer. It is also worth noting that in the presence of the C_{60}SAM, direct electron transfer from the perovskite to the TiO_2 is partially blocked and thus resulted in an improved V_{oc}. This inhibition of electron transfer to the TiO_2 was associated with the energy levels of the components (see inset of Fig. 7a) and poor electronic coupling. Moreover, UV-vis spectra of the films revealed that the addition of the C_{60}SAM does not significantly influence the light absorption of the sensitiser, as shown in Fig. 7a. The charge transport of the TiO_2 was enhanced 4–5 times after the incorporation of the C_{60}SAM. Indeed, the PSCs fabricated in the presence of C_{60}SAM (the device structure is shown in Fig. 7b) exhibited an energy conversion efficiency of

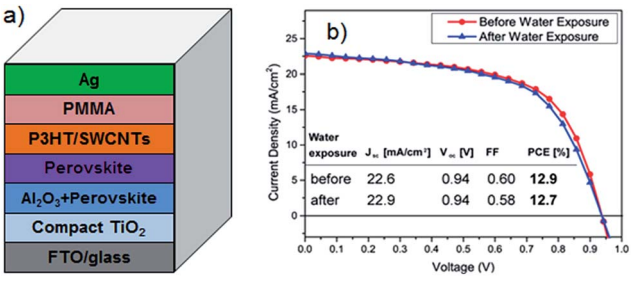

Fig. 6 (a) Schematic illustration of PSC fabricated with CNTs/polymer composite as a hole collection layer as reported by Snaith's group.[79] (b) Current density–voltage curves of PSCs before and after water exposure for 60 s (reprinted with permission from ref. 79 © 2014, American Chemical Society).

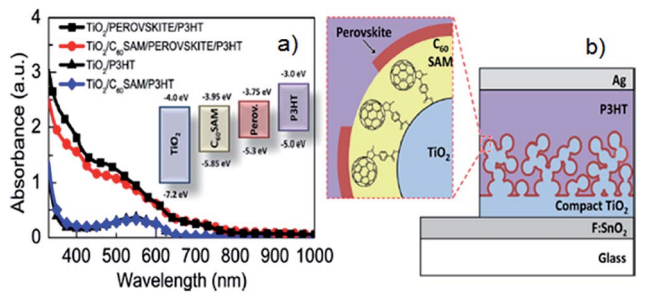

Fig. 7 (a) UV-vis spectra of P_3HT and perovskite films with and without C_{60}SAM. Inset: the energy level of the components used in Snaith's work.[85] (b) The structure of the PSC fabricated with C_{60}SAM layer between perovskite and TiO_2 layers. Reprinted with permission from ref. 85 © 2013, American Chemical Society.

6.7%, which was nearly 2 times higher than that obtained by the benchmark cell (TiO_2/perovskite/P3HT).

A second example is from Zhu *et al.*[81] who synthesised single/few layer GQDs using an electrochemical method such as that illustrated in Fig. 8a and inserted them between the layers of perovskite and TiO_2 nanoparticles. In their PSCs, the GQDs were proposed to serve as a bridge to facilitate electron injection from the perovskite to the TiO_2 conduction band (see Fig. 8b drawn by these authors). However, as shown in Fig. 8b, the conduction band of the GQD (−4.2 eV) is lower than that of the TiO_2 (−4.0 eV). If these energy levels are correct, it is not "downhill" in energy from the perovskite to the GQD to the TiO_2 and hence rapid electron transfer would not seem feasible. However, the final PSC fabricated based on GQDs (Fig. 8c) exhibited a high PCE of 10.15% which was considerably higher than that of GQDs-free cell (8.81%). The authors showed that this significant improvement in the cell performance was associated with the much faster electron injection when GQDs are inserted in the cells. The injection time of electrons from the perovskite to the TiO_2 conduction band was measured to be 260–307 ps using transient absorption spectroscopy. A significant improvement in the electron injection time (90–106 ps) was observed after adding GQDs between the perovskite and TiO_2 layers (see Fig. 8d and e). Although the insertion of GQDs between the perovskite and TiO_2 layers of PSCs has brought a significant improvement in the PV efficiency, the mechanism for this efficiency enhancement clearly needed to be investigated further. In addition, controlling the band gap structure of GQDs for effective electron injection would be a promising future research direction and likely to further improve efficiency of GQDs enhanced PSCs.

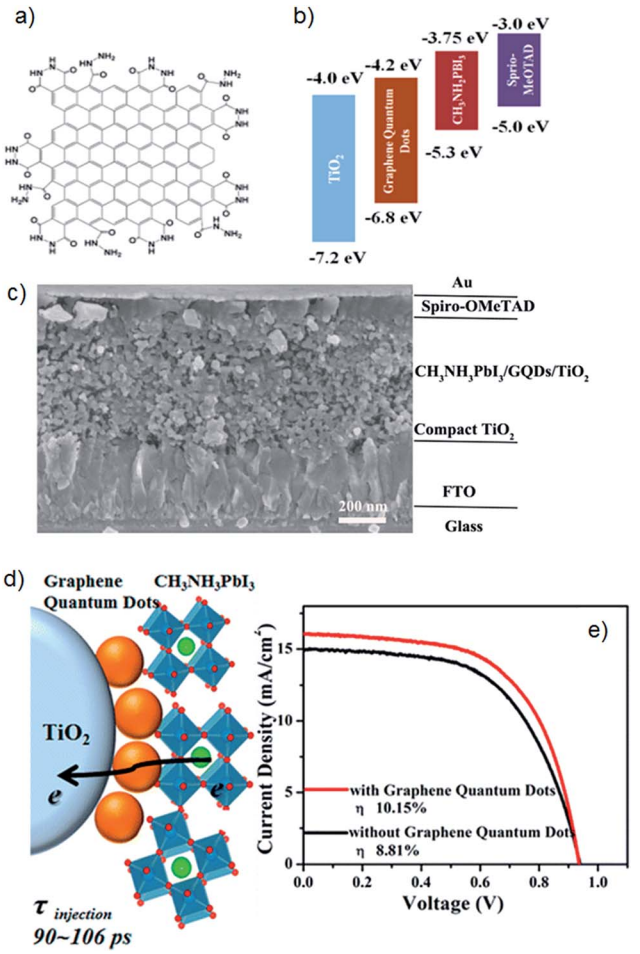

Fig. 8 (a) Schematic of GQD structure. (b) Energy levels of different layers used in PSCs of Zhu *et al.*,[81] (c) Cross sectional SEM image of PSCs fabricated with GQDs. (d) Schematic illustration of electron generation and injection at the interfaces of TiO_2, GQDs and perovskites. (e) Current density–voltage curves for the best performing PSCs. Reprinted with permission from ref. 81 © 2014, American Chemical Society.

Blocking layer (compact layer). The blocking layer (also known as compact layer) is not a major component in liquid-type DSSC but this layer is of particular importance and mandatory for PSCs.[28,29] It is essential to ensure that the blocking layer is pinhole-free and should be uniformly deposited, so that it can prevent charge recombination between the FTO and perovskite or FTO and HTM. In general, the high-temperature processed crystalline TiO_2 blocking layer is an important component to achieve the highest efficiency in PSCs. However, sintering at high temperature has several disadvantages such as slow processing time, high production cost and the limited use with plastic/low melting point substrates. Therefore, inventing a low-temperature processing method is of great interest for the successful development of PSCs. Recently, Wang *et al.*[21] developed low-temperature processed graphene/TiO_2 nanocomposites and employed them as the blocking layers in PSCs. To the best of our knowledge, this study is the first report applying "graphene" in the mesoscopic PSCs and is the only available study to-date that employs carbon nanomaterial in the electron collection layers in PSCs. They prepared graphene/TiO_2 nanocomposite films at temperatures no higher than 150 °C. Notably, a high quality of graphene material is produced in this study using a liquid-phase exfoliation (LPE) method which was previously developed by Hernandez *et al.*[86] and O'Neill *et al.*[87] It was demonstrated that the application of graphene in TiO_2 blocking layer has advantage of not only eliminating the high-temperature processing, it also minimises the series resistance of cells significantly. In the graphene/TiO_2 nanocomposite structure, graphene facilitated a rapid electron transfer within the network and thus suppressed the charge recombination because graphene possesses excellent electrical conductivity. It is well known that graphene-like materials exhibit many fascinating properties especially when they are used as composite structures.[55,88–91] Taking a superiority of synergetic effects between graphene and TiO_2 nanoparticles, the graphene/TiO_2 nanocomposite blocking layer based PSCs achieved very high energy conversion efficiency of 15.6% (under simulated AM 1.5, 106.5 mW cm^{-2} sunlight), which was significantly higher than that (10.0%) obtained by the cell fabricated with the TiO_2-only layer.[21] The full structure of the device that has been used to achieve this highest efficiency (15.6%) is illustrated in Fig. 9a. Moreover, the energy level of graphene is ideal (see Fig. 9b) for the PSCs as its work function sits between the TiO_2 conduction band and FTO and so that the

electrons transfer stepwise from the TiO_2 to FTO without an energy barrier. Furthermore, these authors studied the influence of graphene content in TiO_2 nanoparticles on the cell performance. The efficiency of the cells increased with increasing graphene content ranging from 0 to 0.6 wt%. The optimised graphene loading in the composite was 0.6 wt%, at which the best performance (15.6%) was achieved. However, the cell efficiencies decreased at higher concentrations of graphene. Optimal graphene loadings of 0–1 wt% are commonly observed in graphene composite and hybrid materials[42] and in this case is most likely related to the fact that with higher graphene loading it becomes increasingly likely that direct contact between graphene and perovskite can occur which my will result in recombination centres. It was found by these authors that graphene loading in the nanocomposites does not have significant effect on the light harvesting efficiency (LHE) (see Fig. 9c). Therefore, they confirmed based on the light extinction spectra of each layer of the cell (see Fig. 9d) that the changes in the photocurrent density of the cells were not due to the light absorption characteristic of perovskite layers.

This study[21] suggests that high-efficiency PV cells no longer require a high-temperature sintering process and graphene/TiO_2 nanocomposite materials in PSCs meets the needs of large scale manufacture on a wide range of substrates including plastic films. Therefore, the authors of this review anticipate that many improvements can be made by applying further treatment to the graphene/TiO_2 composite layers. For example, chemical doping is a powerful method to increase the conductivity of graphene.[92] It is reasonable to expect improved performance by incorporating chemically doped graphene in the TiO_2 blocking layers. In addition, CNTs and their well-aligned structures should also be applied in the electron collection layers as they have very unique 1D structure and high conductivity. Furthermore, nanocomposite structures based on graphene and/or CNT materials exhibit extraordinary properties and have been proven to be good candidates for energy applications.[93–95] In particular, CNTs and graphene nanocomposites show special electrical, chemical, physical and catalytic properties. In this regard, the application of CNTs/graphene composites in the TiO_2 blocking layer of PSCs would be an important research direction.

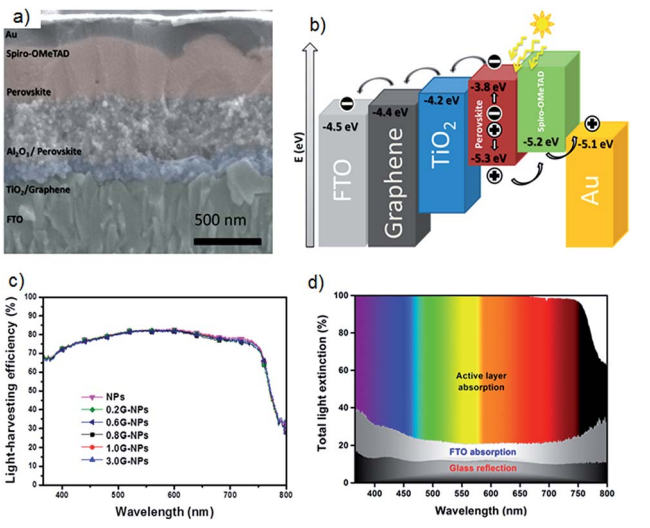

Fig. 9 (a) Cross sectional SEM image of PSC architecture which achieved 15.6% efficiency by Wang *et al.*[21] (b) Schematic illustration of energy levels that shows the work function of graphene is ideally suited for use in this solar cell. (c) Light harvesting efficiency spectra of PSCs as a function of graphene content in the blocking layer. (d) Cumulative light extinction in the low-temperature processed graphene-TiO_2 layer based PSC. Reprinted with permission from ref. 21 © 2014, American Chemical Society.

2.2 Possible applications of carbon materials in PSCs

Transparent conductive oxide. The transparent conductive film (TCF) should be optically transparent to visible light and electrically conductive and is one of the most important components in solar cells. Currently, FTO is the most widely used TCF in PV devices because of its extraordinary electrical properties with a sheet resistance (R_s) = 10–25 Ω sq^{-1} with ~88% transparency. However, FTO films have several disadvantages such as high material cost and scarcity of material. Other major limitations of this film can be their inflexibility, high structural defects and poor stability at high temperature. For these reasons, there has been a rapid growth in the development of FTO alternatives in the past couple of years.[96] TCFs based upon carbon nanomaterials (especially CNTs and graphene) are very promising due to their excellent electrical and mechanical properties, potential low cost and abundance.[41,97–99]

Although CNTs, graphene and their derivatives have been extensively explored in recent years, there are very few reports on using carbon nanomaterials as a TCF for the DSSC window electrode.[100–103] For example, Wei *et al.*[101] reported the fabrication of SWCNTs based polyethylene terephthalate (PET) as a TCF for the DSSC photoelectrode. However, their SWCNTs/PET thin film based DSSC exhibited very poor energy conversion efficiency. Similarly, Kyaw *et al.*[102] also showed that the DSSCs fabricated with the CNTs-TCF based photoelectrodes cannot achieve a good efficiency if no further surface modification is made. These poor efficiencies obtained by the DSSCs fabricated with carbon nanostructures based TCFs are mainly associated with the high catalytic activity of carbon materials for the dissociation of the chemicals involved in the DSSC redox electrolyte. A brief discussion on this phenomenon is as follows: When carbon materials are applied in the photoelectrode, the electrons (injected from the conduction band of semiconducting oxide) recombine with I_3^- in the electrolyte by the reaction $I_3^- + 2e^- \rightarrow 3I^-$, at the electrolyte/photoelectrode interface. Of particular issue here is the limitation of electron transport from the carbon to the external circuit. So, it is difficult to use carbon based TCFs in the photoelectrode of liquid-type solar cells and alternatives should be pursued.

However, it may be possible that TCFs produced from carbon materials can be used as the TCF anode of PSCs because these cells consist of solid electrolyte. In this regard, applying carbon materials based TCFs in PSCs would be very valuable and this could open new avenues of investigation for the researchers leading to advancements such as flexible devices. Many

approaches have been developed to improve the performance of CNTs and graphene based TCFs and they can be found in several recent contributions.[97,98,104–106]

Mesoporous oxide layer. The semiconducting mesoscopic oxide layer plays a critical role in accepting photo-generated electrons from the sensitiser. A good semiconducting layer should be able to simultaneously satisfy the following requirements: (i) the conduction band potential of the semiconductor material must be lower than the excited state of the sensitiser, (ii) have high surface area for maximum sensitiser loading and (iii) have good charge carrier mobility to transport the injected electrons within the network. A wide range of nanostructured semiconducting oxides including TiO_2, Al_2O_3, ZnO, WO_3, ZrO_2 and NiO have been developed for the photoelectrode of PSCs.[24,107–112] Among these semiconducting oxides, nanocrystalline TiO_2 is the most popular and has achieved the highest efficiencies due to its very high surface area-to-volume ratio.[24,113] However, TiO_2 nanoparticles also suffer from several issues such as high rate of charge recombination, slow electron transport and poor light harvesting efficiency. Apart from the development of several nanostructured TiO_2 architectures, semiconducting composites based on carbonaceous materials are promising candidates to address the aforementioned issues. Significant improvements in the DSSC performance have been achieved in past studies by incorporating carbonaceous materials into the TiO_2 photoelectrode and they have been reviewed in our recent review.[114] Similarly, the incorporation of carbon nanostructured materials into the mesoscopic oxide layer of PSCs can be expected to bring remarkable improvement in the cell efficiency. However, the loading of the nanocarbon needs to be optimised to enhance charge transport whilst minimising light absorption and preventing contact between the carbon and HTM to avoid back-transfer of the charges. It is expected that incorporation of nanocarbons into the mesoporous metal oxide layer will be a popular area of research toward high efficiency solar cells.

3 Conclusion and perspectives

In this review, we discussed the progress on the application of carbon based nanomaterials in each aspect of state of the art mesoscopic PSCs. On the basis of recent advancements of PSCs, it is clear that carbon nanomaterials are promising candidates for the development of the PSCs due to their unique properties as well as low cost and abundance. Although excellent achievements have been made in the use of carbon materials in PSCs, this cutting-edge research field is still in its initial stage. Therefore, we expect that the following points will be carefully investigated in the future efforts of using nanocarbons in PSCs.

(i) Carbonaceous materials have been proven to be ideal candidates to replace the precious metal in the cathode of PSCs. Nanocarbon films exhibit the added advantage that they can replace both the metal electrode and HTM. We believe that further improvement in this class of solar cells could be made by upgrading the CNT properties. For instance, the use of pure metallic CNTs would bring critical improvements in the performance of PSCs. Although carbon black and CNTs have been utilised as the PSC cathode, the use of graphene materials in this application is lacking despite graphene possessing higher electrical conductivity than the other forms of carbon. Therefore, reports on using graphene as the conductive cathode of PSCs would be worthwhile. Moreover, chemically doped CNTs and graphene should exhibit very high charge transfer rates. So, applying chemically doped CNTs and graphene in the counter electrode of PSCs would be a promising way to improve the cell performance. Furthermore, the authors of this review anticipate that composite materials based on carbon nanostructures (especially CNTs and graphene) will provide remarkable improvement in the performance of PSCs when they are used in the counter electrode.

(ii) It was found that the carbon materials play a critical role in improving the stability of PSCs. Therefore, additional treatments on CNTs and/or other types of carbon structures would bring significant enhancement. In addition to this, incorporating functionalised CNT structures with other polymers would be an important research direction for the long-term stability of PSCs especially in the hole-transporting layer. The application of graphene and their derivatives in the hole transporting layer of PSCs would be a promising future research direction.

(iii) Inserting GQDs between the perovskite and TiO_2 layers of PSCs was found to be an effective method to improve the PV efficiency of PSCs although the exact mechanism of this improvement is unclear. It is likely that further improvements will be possible by adjusting the band gap of GQDs to optimise electron injection and transfer to the anode.

(iv) Application of graphene in the TiO_2 blocking layer yielded significant improvement in the cell performance. It is well known that chemical doping is an effective approach to enhance the conductivity of graphene material. Based on this concept, improved performance by using chemically doped graphene in the TiO_2 electron collection layers is very likely. In addition, graphene and CNT based composite materials exhibit unique electrical, chemical and physical properties as well as an excellent synergetic effect. For this reason, the use of CNTs/graphene composites in the TiO_2 blocking layer of PSCs would be very valuable for high-performance device.

(v) There is still valuable and important work to be done by exploring the incorporation of carbon materials in the front transparent conductive layer and the mesoporous oxide layer of PSCs. This research would have the potential to further improve the efficiencies and stability of the PSC system.

Acknowledgements

The support of the Australian Research Council Discovery Program (DP130101714) is gratefully acknowledged. Munkhbayar Batmunkh acknowledges International Postgraduate Research Scholarship (IPRS) and Australian Postgraduate Award (APA) for their financial support during his study in Australia.

Notes and references

1 R. F. Service, *Science*, 2005, **309**, 548–551.
2 L. M. Goncalves, V. de Zea Bermudez, H. A. Ribeiro and A. M. Mendes, *Energy Environ. Sci.*, 2008, **1**, 655–667.
3 L. Wang, H. Liu, R. M. Konik, J. A. Misewich and S. S. Wong, *Chem. Soc. Rev.*, 2013, **42**, 8134–8156.
4 B. O'Regan and M. Gratzel, *Nature*, 1991, **353**, 737–740.
5 G. Yu, J. Gao, J. C. Hummelen, F. Wudl and A. J. Heeger, *Science*, 1995, **270**, 1789–1791.
6 M. T. Winkler, W. Wang, O. Gunawan, H. J. Hovel, T. K. Todorov and D. B. Mitzi, *Energy Environ. Sci.*, 2014, **7**, 1029–1036.
7 K. W. J. Barnham and G. Duggan, *J. Appl. Phys.*, 1990, **67**, 3490–3493.
8 S. Mathew, A. Yella, P. Gao, R. Humphry-Baker, F. E. CurchodBasile, N. Ashari-Astani, I. Tavernelli, U. Rothlisberger, K. NazeeruddinMd and M. Grätzel, *Nat. Chem.*, 2014, **6**, 242–247.
9 O. Adebanjo, P. P. Maharjan, P. Adhikary, M. Wang, S. Yang and Q. Qiao, *Energy Environ. Sci.*, 2013, **6**, 3150–3170.
10 C.-C. Chen, W.-H. Chang, K. Yoshimura, K. Ohya, J. You, J. Gao, Z. Hong and Y. Yang, *Adv. Mater.*, 2014, **26**, 5670–5677.
11 W. Wang, M. T. Winkler, O. Gunawan, T. Gokmen, T. K. Todorov, Y. Zhu and D. B. Mitzi, *Adv. Energy Mater.*, 2014, **4**, 1301465.
12 C.-H. M. Chuang, P. R. Brown, V. Bulović and M. G. Bawendi, *Nat. Mater.*, 2014, **13**, 796–801.
13 J. Burschka, N. Pellet, S.-J. Moon, R. Humphry-Baker, P. Gao, M. K. Nazeeruddin and M. Gratzel, *Nature*, 2013, **499**, 316–319.
14 A. Kojima, K. Teshima, Y. Shirai and T. Miyasaka, *J. Am. Chem. Soc.*, 2009, **131**, 6050–6051.
15 J.-H. Im, C.-R. Lee, J.-W. Lee, S.-W. Park and N.-G. Park, *Nanoscale*, 2011, **3**, 4088–4093.
16 H.-S. Kim, C.-R. Lee, J.-H. Im, K.-B. Lee, T. Moehl, A. Marchioro, S.-J. Moon, R. Humphry-Baker, J.-H. Yum, J. E. Moser, M. Gratzel and N.-G. Park, *Sci. Rep.*, 2012, **2**, 591.
17 M. M. Lee, J. Teuscher, T. Miyasaka, T. N. Murakami and H. J. Snaith, *Science*, 2012, **338**, 643–647.
18 J. H. Heo, S. H. Im, J. H. Noh, T. N. Mandal, C.-S. Lim, J. A. Chang, Y. H. Lee, H.-j. Kim, A. Sarkar, K. NazeeruddinMd, M. Gratzel and S. I. Seok, *Nat. Photonics*, 2013, **7**, 486–491.
19 J. H. Noh, S. H. Im, J. H. Heo, T. N. Mandal and S. I. Seok, *Nano Lett.*, 2013, **13**, 1764–1769.
20 M. Liu, M. B. Johnston and H. J. Snaith, *Nature*, 2013, **501**, 395–398.
21 J. T.-W. Wang, J. M. Ball, E. M. Barea, A. Abate, J. A. Alexander-Webber, J. Huang, M. Saliba, I. Mora-Sero, J. Bisquert, H. J. Snaith and R. J. Nicholas, *Nano Lett.*, 2013, **14**, 724–730.
22 S. Ryu, J. H. Noh, N. J. Jeon, Y. Chan Kim, W. S. Yang, J. Seo and S. I. Seok, *Energy Environ. Sci.*, 2014, **7**, 2614–2618.
23 N. J. Jeon, J. H. Noh, Y. C. Kim, W. S. Yang, S. Ryu and S. I. Seok, *Nat. Mater.*, 2014, **13**, 897–903.
24 H. Zhou, Q. Chen, G. Li, S. Luo, T.-b. Song, H.-S. Duan, Z. Hong, J. You, Y. Liu and Y. Yang, *Science*, 2014, **345**, 542–546.
25 P. P. Boix, K. Nonomura, N. Mathews and S. G. Mhaisalkar, *Mater. Today*, 2014, **17**, 16–23.
26 T. C. Sum and N. Mathews, *Energy Environ. Sci.*, 2014, **7**, 2518–2534.
27 P. Gao, M. Gratzel and M. K. Nazeeruddin, *Energy Environ. Sci.*, 2014, **7**, 2448–2463.
28 N.-G. Park, *J. Phys. Chem. Lett.*, 2013, **4**, 2423–2429.
29 N.-G. Park, *Mater. Today*, 2015, **18**, 65–72.
30 G. Hodes, *Science*, 2013, **342**, 317–318.
31 M. A. Green, A. Ho-Baillie and H. J. Snaith, *Nat. Photonics*, 2014, **8**, 506–514.
32 P. Docampo, S. Guldin, T. Leijtens, N. K. Noel, U. Steiner and H. J. Snaith, *Adv. Mater.*, 2014, **26**, 4013–4030.
33 H. J. Snaith, *J. Phys. Chem. Lett.*, 2013, **4**, 3623–3630.
34 B. V. Lotsch, *Angew. Chem., Int. Ed.*, 2014, **53**, 635–637.
35 S. Luo and W. A. Daoud, *J. Mater. Chem. A*, 2015, DOI: 10.1039/c1034ta04953e.
36 M. He, D. Zheng, M. Wang, C. Lin and Z. Lin, *J. Mater. Chem. A*, 2014, **2**, 5994–6003.
37 X. Fan, M. Zhang, X. Wang, F. Yang and X. Meng, *J. Mater. Chem. A*, 2013, **1**, 8694–8709.
38 N. G. Sahoo, Y. Pan, L. Li and S. H. Chan, *Adv. Mater.*, 2012, **24**, 4203–4210.
39 D. Wei and J. Kivioja, *Nanoscale*, 2013, **5**, 10108–10126.
40 L. J. Brennan, M. T. Byrne, M. Bari and Y. K. Gun'ko, *Adv. Energy Mater.*, 2011, **1**, 472–485.
41 J. Du, S. Pei, L. Ma and H.-M. Cheng, *Adv. Mater.*, 2014, **26**, 1958–1991.
42 C. J. Shearer, A. Cherevan and D. Eder, *Adv. Mater.*, 2014, **26**, 2295–2318.
43 D. D. Tune, B. S. Flavel, R. Krupke and J. G. Shapter, *Adv. Energy Mater.*, 2012, **2**, 1043–1055.
44 X. Zhou, J. Qiao, L. Yang and J. Zhang, *Adv. Energy Mater.*, 2014, **4**, 1301523.
45 Z. Yin, J. Zhu, Q. He, X. Cao, C. Tan, H. Chen, Q. Yan and H. Zhang, *Adv. Energy Mater.*, 2014, **4**, 1300574.
46 Q. Li, R. Cao, J. Cho and G. Wu, *Adv. Energy Mater.*, 2014, **4**, 1301415.
47 R. D. Costa, F. Lodermeyer, R. Casillas and D. M. Guldi, *Energy Environ. Sci.*, 2014, **7**, 1281–1296.
48 J. D. Roy-Mayhew and I. A. Aksay, *Chem. Rev.*, 2014, **114**, 6323–6348.
49 H. Wang and Y. H. Hu, *Energy Environ. Sci.*, 2012, **5**, 8182–8188.
50 J. L. Xie, C. X. Guo and C. M. Li, *Energy Environ. Sci.*, 2014, **7**, 2559–2579.
51 J.-K. Sun and Q. Xu, *Energy Environ. Sci.*, 2014, **7**, 2071–2100.
52 X. Cao, Z. Yin and H. Zhang, *Energy Environ. Sci.*, 2014, **7**, 1850–1865.
53 Y.-Y. Lai, Y.-J. Cheng and C.-S. Hsu, *Energy Environ. Sci.*, 2014, **7**, 1866–1883.

54 D. Jariwala, V. K. Sangwan, L. J. Lauhon, T. J. Marks and M. C. Hersam, *Chem. Soc. Rev.*, 2013, **42**, 2824–2860.
55 X. Huang, X. Qi, F. Boey and H. Zhang, *Chem. Soc. Rev.*, 2012, **41**, 666–686.
56 S. Hwang, M. Batmunkh, M. J. Nine, H. Chung and H. Jeong, *ChemPhysChem*, 2015, **16**, 53–65.
57 T. Chen and L. Dai, *J. Mater. Chem. A*, 2014, **2**, 10756–10775.
58 J.-Y. Jeng, Y.-F. Chiang, M.-H. Lee, S.-R. Peng, T.-F. Guo, P. Chen and T.-C. Wen, *Adv. Mater.*, 2013, **25**, 3727–3732.
59 Q. Wang, Y. Shao, Q. Dong, Z. Xiao, Y. Yuan and J. Huang, *Energy Environ. Sci.*, 2014, **7**, 2359–2365.
60 Y. Shao, Z. Xiao, C. Bi, Y. Yuan and J. Huang, *Nat. Commun.*, 2014, **5**, 5784.
61 Z. Wu, S. Bai, J. Xiang, Z. Yuan, Y. Yang, W. Cui, X. Gao, Z. Liu, Y. Jin and B. Sun, *Nanoscale*, 2014, **6**, 10505–10510.
62 Q. Xue, Z. Hu, J. Liu, J. Lin, C. Sun, Z. Chen, C. Duan, J. Wang, C. Liao, W. M. Lau, F. Huang, H.-L. Yip and Y. Cao, *J. Mater. Chem. A*, 2014, **2**, 19598–19603.
63 J.-S. Yeo, R. Kang, S. Lee, Y.-J. Jeon, N. Myoung, C.-L. Lee, D.-Y. Kim, J.-M. Yun, Y.-H. Seo, S.-S. Kim and S.-I. Na, *Nano Energy*, 2015, **12**, 96–104.
64 Z. Ku, Y. Rong, M. Xu, T. Liu and H. Han, *Sci. Rep.*, 2013, **3**, 3132.
65 Y. Rong, Z. Ku, A. Mei, T. Liu, M. Xu, S. Ko, X. Li and H. Han, *J. Phys. Chem. Lett.*, 2014, **5**, 2160–2164.
66 F. Zhang, X. Yang, H. Wang, M. Cheng, J. Zhao and L. Sun, *ACS Appl. Mater. Interfaces*, 2014, **6**, 16140–16146.
67 L. Zhang, T. Liu, L. Liu, M. Hu, Y. Yang, A. Mei and H. Han, *J. Mater. Chem. A*, 2015, DOI: 10.1039/c1034ta04647a.
68 A. Mei, X. Li, L. Liu, Z. Ku, T. Liu, Y. Rong, M. Xu, M. Hu, J. Chen, Y. Yang, M. Grätzel and H. Han, *Science*, 2014, **345**, 295–298.
69 Z. Li, S. A. Kulkarni, P. P. Boix, E. Shi, A. Cao, K. Fu, S. K. Batabyal, J. Zhang, Q. Xiong, L. H. Wong, N. Mathews and S. G. Mhaisalkar, *ACS Nano*, 2014, **8**, 6797–6804.
70 Z. Wei, K. Yan, H. Chen, Y. Yi, T. Zhang, X. Long, J. Li, L. Zhang, J. Wang and S. Yang, *Energy Environ. Sci.*, 2014, **7**, 3326–3333.
71 L. Qiu, J. Deng, X. Lu, Z. Yang and H. Peng, *Angew. Chem., Int. Ed.*, 2014, **53**, 10425–10428.
72 M. Xu, Y. Rong, Z. Ku, A. Mei, T. Liu, L. Zhang, X. Li and H. Han, *J. Mater. Chem. A*, 2014, **2**, 8607–8611.
73 M. Hu, L. Liu, A. Mei, Y. Yang, T. Liu and H. Han, *J. Mater. Chem. A*, 2014, **2**, 17115–17121.
74 M. S. Arnold, A. A. Green, J. F. Hulvat, S. I. Stupp and M. C. Hersam, *Nat. Nanotechnol.*, 2006, **1**, 60–65.
75 D. D. Tune, F. Hennrich, S. Dehm, M. F. G. Klein, K. Glaser, A. Colsmann, J. G. Shapter, U. Lemmer, M. M. Kappes, R. Krupke and B. S. Flavel, *Adv. Energy Mater.*, 2013, **3**, 1091–1097.
76 F. Fabregat-Santiago, J. Bisquert, L. Cevey, P. Chen, M. Wang, S. M. Zakeeruddin and M. Grätzel, *J. Am. Chem. Soc.*, 2008, **131**, 558–562.
77 A. Abate, T. Leijtens, S. Pathak, J. Teuscher, R. Avolio, M. E. Errico, J. Kirkpatrik, J. M. Ball, P. Docampo, I. McPherson and H. J. Snaith, *Phys. Chem. Chem. Phys.*, 2013, **15**, 2572–2579.
78 J. Burschka, A. Dualeh, F. Kessler, E. Baranoff, N.-L. Cevey-Ha, C. Yi, M. K. Nazeeruddin and M. Grätzel, *J. Am. Chem. Soc.*, 2011, **133**, 18042–18045.
79 S. N. Habisreutinger, T. Leijtens, G. E. Eperon, S. D. Stranks, R. J. Nicholas and H. J. Snaith, *Nano Lett.*, 2014, **14**, 5561–5568.
80 S. Iijima, *Nature*, 1991, **354**, 56–58.
81 Z. Zhu, J. Ma, Z. Wang, C. Mu, Z. Fan, L. Du, Y. Bai, L. Fan, H. Yan, D. L. Phillips and S. Yang, *J. Am. Chem. Soc.*, 2014, **136**, 3760–3763.
82 G. Xing, N. Mathews, S. Sun, S. S. Lim, Y. M. Lam, M. Grätzel, S. Mhaisalkar and T. C. Sum, *Science*, 2013, **342**, 344–347.
83 K. J. Williams, C. A. Nelson, X. Yan, L.-S. Li and X. Zhu, *ACS Nano*, 2013, **7**, 1388–1394.
84 Z. Zhang, J. Zhang, N. Chen and L. Qu, *Energy Environ. Sci.*, 2012, **5**, 8869–8890.
85 A. Abrusci, S. D. Stranks, P. Docampo, H.-L. Yip, A. K. Y. Jen and H. J. Snaith, *Nano Lett.*, 2013, **13**, 3124–3128.
86 Y. Hernandez, V. Nicolosi, M. Lotya, F. M. Blighe, Z. Sun, S. De, I. T. McGovern, B. Holland, M. Byrne, Y. K. Gun'Ko, J. J. Boland, P. Niraj, G. Duesberg, S. Krishnamurthy, R. Goodhue, J. Hutchison, V. Scardaci, A. C. Ferrari and J. N. Coleman, *Nat. Nanotechnol.*, 2008, **3**, 563–568.
87 A. O'Neill, U. Khan, P. N. Nirmalraj, J. Boland and J. N. Coleman, *J. Phys. Chem. C*, 2011, **115**, 5422–5428.
88 K. S. Novoselov, A. K. Geim, S. V. Morozov, D. Jiang, Y. Zhang, S. V. Dubonos, I. V. Grigorieva and A. A. Firsov, *Science*, 2004, **306**, 666–669.
89 K. S. Novoselov, A. K. Geim, S. V. Morozov, D. Jiang, M. I. Katsnelson, I. V. Grigorieva, S. V. Dubonos and A. A. Firsov, *Nature*, 2005, **438**, 197–200.
90 A. K. Geim and K. S. Novoselov, *Nat. Mater.*, 2007, **6**, 183–191.
91 R. R. Nair, P. Blake, A. N. Grigorenko, K. S. Novoselov, T. J. Booth, T. Stauber, N. M. R. Peres and A. K. Geim, *Science*, 2008, **320**, 1308.
92 F. Schedin, A. K. Geim, S. V. Morozov, E. W. Hill, P. Blake, M. I. Katsnelson and K. S. Novoselov, *Nat. Mater.*, 2007, **6**, 652–655.
93 Y. Sun, Q. Wu and G. Shi, *Energy Environ. Sci.*, 2011, **4**, 1113–1132.
94 D. Chen, H. Zhang, Y. Liu and J. Li, *Energy Environ. Sci.*, 2013, **6**, 1362–1387.
95 H. Chang and H. Wu, *Energy Environ. Sci.*, 2013, **6**, 3483–3507.
96 K. Ellmer, *Nat. Photonics*, 2012, **6**, 809–817.
97 S. Roth and H. J. Park, *Chem. Soc. Rev.*, 2010, **39**, 2477–2483.
98 L. Hu, D. S. Hecht and G. Grüner, *Chem. Rev.*, 2010, **110**, 5790–5844.
99 J. K. Wassei and R. B. Kaner, *Mater. Today*, 2010, **13**, 52–59.
100 X. Wang, L. Zhi and K. Müllen, *Nano Lett.*, 2007, **8**, 323–327.
101 D. Wei, H. S. Unalan, D. Han, Q. Zhang, L. Niu, G. Amaratunga and T. Ryhanen, *Nanotechnology*, 2008, **19**, 424006.

102 A. K. K. Kyaw, H. Tantang, T. Wu, L. Ke, C. Peh, Z. H. Huang, X. T. Zeng, H. V. Demir, Q. Zhang and X. W. Sun, *Appl. Phys. Lett.*, 2011, **99**, 021107.
103 J. Du, F. Bittner, D. S. Hecht, C. Ladous, J. Ellinger, T. Oekermann and M. Wark, *Thin Solid Films*, 2013, **531**, 391–397.
104 D. S. Hecht, L. Hu and G. Irvin, *Adv. Mater.*, 2011, **23**, 1482–1513.
105 Q. Zheng, Z. Li, J. Yang and J.-K. Kim, *Prog. Mater. Sci.*, 2014, **64**, 200–247.
106 S. B. Yang, B.-S. Kong, D.-H. Jung, Y.-K. Baek, C.-S. Han, S.-K. Oh and H.-T. Jung, *Nanoscale*, 2011, **3**, 1361–1373.
107 J.-Y. Jeng, K.-C. Chen, T.-Y. Chiang, P.-Y. Lin, T.-D. Tsai, Y.-C. Chang, T.-F. Guo, P. Chen, T.-C. Wen and Y.-J. Hsu, *Adv. Mater.*, 2014, **26**, 4107–4113.
108 T. Leijtens, G. E. Eperon, S. Pathak, A. Abate, M. M. Lee and H. J. Snaith, *Nat. Commun.*, 2013, **4**, 2885.
109 M. H. Kumar, N. Yantara, S. Dharani, M. Graetzel, S. Mhaisalkar, P. P. Boix and N. Mathews, *Chem. Commun.*, 2013, **49**, 11089–11091.
110 K. Mahmood, B. S. Swain, A. R. Kirmani and A. Amassian, *J. Mater. Chem. A*, 2015, DOI: 10.1039/c1034ta04883k.
111 D. Bi, S.-J. Moon, L. Haggman, G. Boschloo, L. Yang, E. M. J. Johansson, M. K. Nazeeruddin, M. Gratzel and A. Hagfeldt, *RSC Adv.*, 2013, **3**, 18762–18766.
112 K.-C. Wang, J.-Y. Jeng, P.-S. Shen, Y.-C. Chang, E. W.-G. Diau, C.-H. Tsai, T.-Y. Chao, H.-C. Hsu, P.-Y. Lin, P. Chen, T.-F. Guo and T.-C. Wen, *Sci. Rep.*, 2014, **4**, 4756.
113 A. K. Chandiran, M. Abdi-Jalebi, M. K. Nazeeruddin and M. Grätzel, *ACS Nano*, 2014, **8**, 2261–2268.
114 M. Batmunkh, M. J. Biggs and J. G. Shapter, *Adv. Sci.*, 2015, **2**, 201400025.